(ddd, 1 H, $NCH_2CH_2CHH$, $J$ = 7, 7, 16 Hz), 2.54 (ddd, 1 H, $NCH_2CH_2CHH$, $J$ = 7, 7, 16 Hz), 3.61 (m, 2 H, $NCH_2$), 4.05 (s, 3 H, $OCH_3$), 4.07 (q, 2 H, $CH_2CH_3$), 8.7 (br, 1 H, NH); IR (neat) 3378, 2985, 1658, 1582 $cm^{-1}$; mass spectrum $m/e$ (rel intensity) 387 (3.5, M + $2^{81}Br$), 385 (8.3, M + $2^{79}Br$ and $M^{+81}Br$), 383 (5.0, $M^{+79}Br$, 341, 339 (8.8, 8.9), 326, 324 (19.4, 19.7), 304 (100), 276 (82.1), 258 (18.9), 246 (11.0), 230 (10.9).

**Air Oxidation of Hydroquinone 29 to Quinone 27.** A 15-mg sample of **29** partially air oxidized over the course of ~1 month. Purification of **29** (1 g of $SiO_2$: solvent 1) provided a small sample of pure **27**: $R_f$ (solvent 1) 0.28; NMR ($CDCl_3$) $\delta$ 1.16 (t, 3 H, $CH_2CH_3$, $J$ = 7 Hz), 2.00 (s, 3 H, $CH_3$), 2.0 (masked m, 2 H, $NCH_2CH_2$), 2.31 (ddd, 1 H, $NCH_2CH_2CHH$, $J$ = 8, 8, 17 Hz), 2.62 (ddd, 1 H, $NCH_2CH_2CHH$, $J$ = 8, 8, 17 Hz), 3.62 (m, 2 H, $NCH_2$), 4.01 (s, 3 H, $OCH_3$), 4.06 (q, 2 H, $CH_2CH_3$), 8.7 (br, 1 H, NH); IR (neat) 3325, 1675, 1661, 1650, 1591, 1573 $cm^{-1}$.

**Metal-Catalyzed Cyclization of Hydroquinone 29 to Indoloquinone 16.** To a stirred solution of **29** (8.0 mg, 0.02 mmol) in acetonitrile (0.42 mL) were added $K_2CO_3$ (9.0 mg, 0.6 mmol, 320 mol %) and $CuBr_2$ (1.0 mg, 0.005 mmol, 20 mol %). Oxidation to purple **27** was seen within minutes. After 11 h the yellow mixture was filtered and evaporated. The residue was dissolved in chloroform, filtered, and evaporated to give **16** as a yellow solid (6.3 mg, 98%), identical with the material prepared above.

**Metal-Catalyzed Cyclization of Hydroquinone 28 to Indoloquinone 30.** The above reaction was repeated on the same scale using hydroquinone **28**. Isolation after 4.5 h gave **30**: 6.3 mg (98%), mp 157-159 °C; $R_f$ (solvent I) 0.56; $R_t$ (column A, solvent G, 2 mL/min) 23.7; NMR ($CDCl_3$) 1.38 (t, 3 H, $CH_2CH_3$, $J$ = 7.1 Hz), 2.01 (s, 3 H, $CH_3$), 2.60 (tt, 2 H, $NCH_2CH_2$), 3.12 (t, 2 H, $NCH_2CH_2CH_2$, $J$ = 7.6), 3.97 (s, 3 H, $OCH_3$), 4.31 (masked t, 2 H, $NCH_2$, $J$ = 7.4 Hz), 4.34 (q, 2 H, $CH_2CH_3$); IR ($CHCl_3$) 2985, 1727, 1695, 1661, 1616, 1504, 1374, 1319, 1302, 1200, 1129, 1096, 1009, 933 $cm^{-1}$. Anal. Calcd for $C_{16}H_{17}NO_5$: C, 63.3; H, 5.6; N, 4.6. Found: C, 63.2; H, 5.8; N, 4.6.

**Addition of Vinylogous Carbamate 25 to Quinone 7 in the Presence of Copper. Ring Closure to Indoloquinone 3 Esters 16 and 30.** To a rapidly stirred solution of **7** (50 mg, 0.16 mmol) and **25** (25 mg, 0.16 mmol) in acetonitrile (2 mL) were added $K_2CO_3$ (78 mg, 0.56 mmol, 350 mol %), and $CuBr_2$ (3.6 mg, 0.016 mmol, 10 mol %). After 5 days, the mixture was filtered and evaporated to a yellow solid (50 mg, 102%). NMR ($CDCl_3$) analysis showed **16** and **30** in a ratio of 5/95. Preparative MPLC (solvent H) of 10 mg of the mixture gave base-line separation of **16** and **30** and a recovery of 9 mg of **30**.

**Registry No. 4**, 2207-57-0; **7**, 77357-44-9; **8**, 85096-93-1; **9**, 85083-28-9; **10**, 85083-29-0; (*E*)-**11**, 85083-30-3; **12a**, 85083-31-4; **12b**, 85083-32-5; (*E*)-**13**, 85096-94-2; **14**, 85083-33-6; (*E*)-**15**, 85083-34-7; **16**, 83605-97-4; **17**, 83605-95-2; **18**, 3188-26-9; **19**, 29769-40-2; **20**, 66865-11-0; (*E*)-**21**, 85083-35-8; **22**, 85083-36-9; **23**, 85083-37-0; **24**, 85083-38-1; (*Z*)-**25**, 35150-22-2; (*Z*)-**26**, 85083-39-2; (*Z*)-**27**, 85083-40-5; (*Z*)-**28**, 85083-41-6; (*Z*)-**29**, 85083-42-7; **30**, 85083-43-8; $Mg(O_2CCH_2CO_2C_2H_5)_2$, 37517-78-5; 2-methoxy-3-methylhydroquinone, 1760-80-1; 2,3-dibromo-5-methoxy-6-methylhydroquinone, 77357-50-7; homoproline ethyl ester acetate salt, 72866-98-9; 4-aminobutyric acid, 56-12-2.

# Nitric Oxide Ferrohemes: Kinetics of Formation and Photodissociation Quantum Yields

**Emily J. Rose and Brian M. Hoffman***

*Contribution from the Department of Chemistry, Northwestern University, Evanston, Illinois 60201.* *Received August 5, 1982*

**Abstract:** The quantum yield for NO photodissociation from iron protoporphyrin 1-methylimidazole nitrosyl, FePP(1-MeIm)(NO), in the presence of excess 1-MeIm is wavelength independent, $\Phi_1$ = 0.08-0.1, and the NO binding rate to the five-coordinate heme, Fe(PP)(1-MeIm), is $k_5^{NO} = 1.7 \pm 0.7 \times 10^8$ $M^{-1}$ $s^{-1}$; for Fe(PP)(NO), $\Phi_1$ = 0.05-0.08. This quantum yield is much higher than believed earlier but nevertheless appears to be significantly less than unity; the result is important to an understanding of heme-ligand photodissociation. In contrast for myoglobin and T- and R-state hemoglobin, $k_5 = 1.8 \times 10^7$ $M^{-1}$ $s^{-1}$ and $\Phi_1 = 10^{-3}$. The observations for model systems and proteins (and comparable results for CO) can be understood self-consistently within a scheme for ligand binding and photorelease that incorporates as an intermediate a (heme, ligand) encounter pair, in the one case surrounded by a solvent cage and in the other embedded in the heme pocket of a protein. At ambient temperature, dissociation of a (heme model, NO) encounter pair in solution is several times more likely than bond formation. In contrast, because diffusion into and out of the protein heme pocket is restricted, a NO molecule in the pocket is over 100 times more likely to bind than to escape.

We have employed flash photolytic techniques to measure the quantum yields for NO photodissociation from nitrosylferroheme model compounds and the rate constant for NO binding to the five-coordinate $Fe^{II}PP$(1-MeIm).[1] Comparisons between results for model compounds and those for hemoproteins are particularly useful in examining the mechanisms by which the properties of the heme group are modulated by a protein environment.[2-4] The binding of NO by ferrohemoproteins is anomalous in a number of respects. Although cooperatively is shown in the binding of $O_2$ and CO to Hb,[5] the association of NO is noncooperative.[6,7] The kinetics of CO binding to R- and T-state Hb exhibits allosteric differentiation, with further differentiation in Mb,[8,9] but all three binding rates are identical for NO.[7,10] Finally, the binding rate of CO to unconstrained model hemes is identical with that of R-state hemoglobin,[11,9] whereas a preliminary report by Morris and Gibson suggests that the rate of NO binding in the protein is depressed.[10] We find that both the NO photodissociation quantum yield and binding rates for the heme model FePP(1-

(1) Abbreviations: FePP, ferrous protoporphyrin(IX); 1-MeIm, 1-methylimidazole; Hb, hemoglobin; T, low affinity; R, high affinity; Mb, myoglobin; CTAB, cetyltrimethylammonium bromide; L, diatomic ligand; B, nitrogenous base.

(2) (a) Traylor, T. *Acc. Chem. Res.* **1981**, *14*, 102-109, and references therein. (b) Geibel, J.; Cannon, J.; Campbell, D.; Traylor, T. G. *J. Am. Chem. Soc.* **1978**, *100*, 3575-3585.

(3) Hoffman, B.; Swartz, J.; Stanford, M.; Gibson, Q. *Adv. Chem. Ser.* **1980**, *No. 191*, 235-252.

(4) Hashimoto, T.; Dyer, R. C.; Crossley, M. J.; Baldwin, J. E.; Basolo, F. *J. Am. Chem. Soc.* **1982**, *104*, 2101-2109.

(5) Anderson, S. R.; Antonini, E. *J. Biol. Chem.* **1968**, *243*, 2918.

(6) Cassoly, R.; Gibson, Q. H. *J. Mol. Biol.* **1975**, *91*, 301-313.

(7) Moore, E. G.; Gibson, Q. H. *J. Biol. Chem.* **1976**, *251*, 2788-2794.

(8) Antonini, E.; Brunori, M. "Hemoglobin and Myoglobin in Their Reactions with Ligands"; North Holland: Amsterdam, 1971; pp 226.

(9) Blough, N. V.; Hoffman, B. M. *J. Am. Chem. Soc.* **1982**, *104*, 4247.

(10) Morris, R. J.; Gibson, Q. H. *J. Biol. Chem.* **1980**, *255*, 8050-8053.

(11) Rose, E. J.; Venkatasubramian, P. N.; Swartz, J. C.; Jones, R. D.; Basolo, F.; Hoffman, B. M. *Proc. Natl. Acad. Sci. U.S.A.* **1982**, *79*, 5742-5745.

0002-7863/83/1505-2866$01.50/0 

MeIm) are much larger than those for Hb.[12] The observations for proteins and heme models can be understood self-consistently within a scheme for ligand binding and photorelease that includes as an intermediate a (heme, ligand) encounter pair, respectively, surrounded by a solvent cage or embedded in the heme pocket of a protein. The difference between results for hemoprotein and model arises because a ligand can only enter or exit the heme pocket through a restricted pathway;[13] elaborate mechanisms of protein control are not involved in NO binding.

Ligand photorelease has been examined for a wide variety of hemes, hemoproteins, and their analogues, but the nature of this process is not yet fully clarified.[14-17] Hoffman and Gibson considered the photolability of a range of metalloporphyrin–ligand systems and suggested a classification scheme in which those having a total occupancy ($r$) of the metal d orbitals and ligand $\pi^*$ orbitals of $r = 6$ were highly photolabile, while those with $r \geq 7$ were not.[14] However, as they anticipated, subsequent work on the nanosecond and picosecond times scales indeed indicates that ligand photorelease quantum yields measured on microsecond time scales or longer may be underestimated because of geminate recombination or rapid second-order recombination of photofragments.[18,19] For example, nitrogeneous base complexes of ferrohemes formerly were regarded as totally photoinert but now have been observed to photodissociate[19] with quantum yields $\Phi \sim 10^{-1}$–$10^{-2}$, and with second-order recombination rates of $10^8$–$10^9$ $M^{-1}$ $s^{-1}$. Since NO also binds rapidly, it was thus of considerable importance to reevaluate the apparently low quantum yield for photorelease of NO from the $r = 7$ nitrosylferroheme model compounds, $\Phi_1^{NO}$.[12,14] By the proper choice of solution conditions, namely, high concentration of an appropriate nitrogenous base and low concentration of NO, we have been able to trap the ferroheme product of NO photodissociation as a nitrogenous base adduct, which permits us to measure $\Phi_1^{NO}$ without artifactual reduction by second-order recombination processes.

## Experimental Section

**Materials.** Hemin (bovine, type I) was used as received from Sigma. 1-Methylimidazole (Aldrich, 99%) was distilled from sodium metal and stored over KOH. 2-Methylimidazole (Aldrich, 99%) was recrystallized prior to use. Nitric oxide (Matheson C. P., 99%) was passed through a 2 × 30 cm column of solid KOH prior to use in order to remove higher oxides. Horseheart myglobin (Mb) was used as received from Sigma. Cetyltrimethylammonium bromide (CTAB) was used as received from Sigma.

**Apparatus.** Flash photolysis was performed on an apparatus previously described.[20] Actinic light normally was provided by an Electrophotonics pulsed dye laser (unmodelocked) with rhodamine-6-G (R6G) in methanol as the active medium. In some cases, it was convenient to employ a Sunpak 611 photographic flash, screened by appropriate Corning colored glass filters, as the photolysis source. In order to examine the wavelength dependence of the quantum yield for photodissociation, we used a National Research Group pulsed-nitrogen laser (λ 337.1 nm) for photolysis to the blue of the Soret peak.

**Sample Preparation.** Samples were prepared either in tonometers, with large vapor/liquid volume ratios, or in cells designed for all-liquid samples, which consisted of cuvettes to which 8-mm o.d. tubing had been attached.[21] All manipulations were performed with airless syringes.

**FePP(1-MeIm)(NO).** Stock solutions of $Fe^{III}PP(1\text{-MeIm})_2$ were prepared by dissolving hemin chloride in aqueous Tris·HCl buffer (pH 9) containing at least 20% (v/v) 1-MeIm. Romberg and Kassner found this base concentration necessary in order to insure that only the six-coordinate FePP(1-MeIm)(NO) complex is present when NO is added[22]; a high base concentration is also required in order to observe NO photolysis and rebinding as predicted by Scheme I (see below). The stock solution was degassed by bubbling with $N_2$ for 30 min before addition to a prepurged cell. Stock solutions of NO-saturated 1-MeIm were prepared by subjecting the base to three freeze–pump–thaw cycles and then bubbling the solution with NO (in a hood) for 15 min prior to use.

An aliquot of the NO-saturated 1-MelM was removed from the stock under NO purge and injected into the $Fe^{III}PP(1\text{-MeIm})_2$ sample. Reduction to the $Fe^{II}PP(1\text{-MeIm})(NO)$ species occurred promptly, and its spectrum agreed with that previously reported for FePP(1-MeIm)(NO) ($\lambda_{max}$ 415 nm, Figure 1).[22] In order to verify that both the unliganded and liganded ferroheme species were present in monomeric form, spectra of the two species were recorded in the presence of 2% CTAB. This detergent prevents aggregation of the model hemes in solution.[2b] Spectra recorded with and without CTAB were identical in all cases.

The $Fe^{II}$–NO species was slowly oxidized, in 1–2 h, by oxygen diffusion through the rubber septum. A double-septum arrangement was used in order to prevent this. After addition of NO-saturated base, a second rubber septum was inserted into the neck of the sample cell. The space between the two stoppers was evacuated and refilled with $N_2$ 2–3 times. Approximately 100 μL of aqueous sodium dithionite (1.5 M) was injected into the space between the two stoppers to serve as a barrier to oxygen diffusion. NO can also diffuse out of the sample, reducing [NO] and lowering rebinding rates. The usable sample lifetime for a quantum yield determination (which does not require accurate knowledge of [NO] or accurate rates) was increased to ~8 h by the dual-septum arrangement. However, measurements of the rebinding kinetics of NO with the porphyrin were made within the first 15 min after sample preparation.

**FePP(NO).** $Fe^{III}PP$ in degassed buffer (pH 9) was placed in a tonometer. Addition of solid $Na_2S_2O_4$ followed by NO purge yielded $Fe^{II}PP(NO)$. Alternatively, the addition of dithionite could be omitted and autoreduction by NO allowed to proceed. The absorption spectra from samples produced by both methods were identical. All-liquid samples of FePP(NO) in 2-MeIm solution (0.5–2.0 M in pH 9 buffer) were prepared in a similar manner to that described for FePP(1-MeIm)(NO).

**Equilibrium Measurements.** Affinity constants for the formation of the mono(base) and bis(base) adducts of $Fe^{II}PP$, $K_1$ and $K_2$, were obtained by using the method of Brault and Rougee.[23] The reduced four-coordinate porphyrin (typically $1\text{–}2 \times 10^{-5}$ M; $\epsilon_{FePP}$ $6.9 \times 10^4$ $M^{-1}$ $cm^{-1}$ at 436.8 nm[22]) in 2% CTAB solution (50 mM Tris·HCl, pH 9) was titrated with 1-MeIm, and absorbance changes were monitored at 436.8 nm, an isosbestic point for $FePP(B)_2$ and FePP. Titrations with 2-MeIm gave the extinction coefficients of Fe(PP)(2-MeIm), since the bis(base) adduct does not form.

The solubility of NO has been measured in water (2 mM/atm)[24] and in a variety of organic solvents (e.g., toluene, 11 mM/atm)[24] but not in 1-methylimidazole or other nitrogenous bases. The concentration of NO present in NO-saturated 1-MeIm was measured with the following procedure. A stock solution of sodium dithionite was prepared in buffer (Tris, pH 9) and standardized by optical titration of methylene blue ($\epsilon$ $6.64 \times 10^4$ $M^{-1}$ $cm^{-1}$ at 665 nm[25]). The dithionite extinction coefficient at 316 nm was found to be $4.8 \times 10^3$ $M^{-1}$ $cm^{-1}$. An all-liquid sample of the dithionite solution in water was prepared by using the same procedure as that for the $FePP(1\text{-MeIm})_2$ samples. Aliquots of NO-saturated 1-MeIm were added and the successive absorbances at 316 nm recorded.

The solubility of CO in 30% (v/v) 1-MeIm in aqueous buffer (Tris, pH 9) was obtained by titrating a sample of reduced Mb in aqueous buffer with aliquots of the CO-saturated 30% 1-MeIm/buffer solution. The formation of MbCO was monitored at the Soret maximum (λ 423.5 nm).[8]

**Quantum Yields.** Quantum yields were determined relative to MbCO ($\Phi = 1$) as previously described.[20] For Fe(Por)(B)(CO) systems:

$$-\ln\left(1 - \frac{\Delta A_0(I)}{\Delta A_0(\infty)}\right) = \omega I \qquad (1)$$

describes the relationship between the degree of photolysis and the intensity of the photolytic flash.[26] $\Delta A_0(\infty)$ is the zero-time absorbance

(12) Saffran, W. A.; Gibson, Q. H. *J. Biol. Chem.* **1977**, *252*, 7955–7958.
(13) Szabo, A. *Proc. Natl. Acad. Sci. U.S.A.* **1978**, *75*, 2108–2111.
(14) Hoffman, B. M.; Gibson, Q. H. *Proc. Natl. Acad. Sci. U.S.A.* **1978**, *75*, 21–25.
(15) Stanford, M. A.; Hoffman, B. M. *J. Am. Chem. Soc.* **1981**, *103*, 4104–4113.
(16) Reynolds, A. H.; Rand, S. D.; Rentzepis, P. M. *Proc. Natl. Acad. Sci. U.S.A.* **1981**, *78*, 2292–2296.
(17) Cornelius, P. A.; Steele, A. W.; Chernoff, D. A.; Hochstrasser, R. M. *Proc. Natl. Acad. Sci. U.S.A.* **1981**, *78*, 7526–7529.
(18) (a) Duddell, D.; Morris, R. J.; Muttucumaru, N. J.; Richards, J. T. *Photochem. Photobiol.* **1980**, *31*, 479–484. (b) Duddell, D. A.; Morris, R. J.; Richards, J. T. *Biochem. Biophys. Acta* **1980**, *621*, 1–8.
(19) Lavalette, D.; Tetreau, C.; Momenteau, M. *J. Am. Chem. Soc.* **1979**, *101*, 5395–5401.
(20) Stanford, M. A.; Swartz, J. C.; Phillips, T. E.; Hoffman, B. M. *J. Am. Chem. Soc.* **1980**, *102*, 4492–4499.
(21) Traylor, T. G.; Chang, C. K.; Geibel, J.; Berzinis, A.; Mincey, T.; Cannon, J. *J. Am. Chem. Soc.* **1979**, *101*, 6716–6731.
(22) Romberg, R. W.; Kassner, R. J. *Biochemistry* **1979**, *18*, 5387–5392.
(23) Brault, D.; Rougee, M. *Biochem. Biophys. Res. Commun.* **1974**, *57*, 654–659.
(24) (a) Shaw, A. W.; Vosper, A. J. *J. Chem. Soc., Faraday Trans. 1* **1977**, *73*, 1239–1244. (b) Linke, W. F.; Seidell, A. "Solubilities of Inorganic and Metal–Organic Compounds"; Van Nostrand: Princeton, NJ, 1958; pp 453–459, 790–792.
(25) Ho, P. S., unpublished results.

Table I. Equilibrium Binding Constants, $K_L$, for NO and CO Binding to Hemes and Hemoproteins

| heme | $P_{1/2}{}^{L}$,[a] torr | | $K_L$,[b] $M^{-1}$ | | $K_{NO}/K_{CO}$ |
|---|---|---|---|---|---|
| | NO | CO | NO | CO | |
| FePP(1-MeIm) | $5.7 \times 10^{-7}$ | $1.2 \times 10^{-3}$ | $5.8 \times 10^{11}$ | $7.8 \times 10^{8}$ | 740 |
| Mb | $1.1 \times 10^{-6}$ | $1.8 \times 10^{-2}$ | $3.4 \times 10^{11}$ | $4.5 \times 10^{7}$ | 7500 |
| Hb | $1.5 \times 10^{-5}$ | $3.5 \times 10^{-2}$ | $2.5 \times 10^{10}$ | $2.3 \times 10^{7}$ | 1100 |

[a] $P_{1/2}$ values for FePP(1-MeIm) 20% 1-MeIm (v/v) from Romberg and Kassner, ref 22. $P_{1/2}$ values for Mb and Hb from Antonini and Brunori, ref 8. [b] Equilibrium constants calculated by using $K_L = (s_L P_{1/2}{}^{L})^{-1}$ (L = CO, NO). For 20% 1-MeIm (v/v), aqueous buffer, we estimate $s_{NO}$ = 3 mM/atm in neat 1-MeIm (see text) and $s_{NO}$ = 2 mM/atm in $H_2O$.[24] For 30% 1-MeIm (v/v), aqueous buffer, $s_{CO}$ = 0.8 mM/atm (see text). For Hb and Mb (L = CO, NO), solubilities in water[24] are $s_{NO}$ = 2 mM/atm, $s_{CO}$ = 0.94 mM/atm.

change upon full photolysis, $\Delta A_0(I)$ is the zero-time absorbance change for a flash with total photon flux incident on the sample $I$, and $\omega$ is a constant proportional to the photorelease quantum yield and for a monochromatic excitation source is given by the expression:

$$\omega = \Phi(\lambda)\epsilon(\lambda)i(\lambda) \quad (2)$$

Here $i(\lambda)$ is the fractional photon flux of the photolytic flash source with wavelength $\lambda$, $\epsilon(\lambda)$ is the extinction of the sample, and $\Phi(\lambda)$ is the quantum yield at the wavelength of excitation. For CO photorelease in MbCO, $\Phi$ = 1 at all wavelengths,[12] and so MbCO can be used as a reference for any source of actinic light. In the case of a nonmonochromatic source, eq 2 must be integrated over the wavelength range illuminated by source. When the actinic source is screened by a sequence of neutral density filters, a plot of the left-hand side of eq 1 vs. the relative intensity of the source yields a straight line with slope $\omega$. $\Phi_{NO}$ may be obtained by comparison of $\omega_{NO}$ and $\omega_{CO}$ after the differences in extinction profile are taken into account.

The nitrogen laser is monochromatic with a 0.1-nm bandwidth centered at 337.1 nm. The dye laser emission is effectively monochromatic; the profile, obtained by monitoring the intensity of light scattered from an empty cuvette placed in the flash apparatus, covered a narrow wavelength band (±10 nm) with the emission maximum at 590 nm. The photographic flash was screened by a Corning 3-71 sharp cut yellow filter (40% transmittance at 480 nm) and has a relatively flat output over the porphyrin $\alpha$–$\beta$ absorbance region.

## Results

**Reference Equilibrium Measurements.** Analysis of the kinetics of ligand binding to Fe(PP) requires a knowledge of the equilibrium constants for 1-MeIm binding to the porphyrin and of the NO or CO concentration in the sample solution (see Scheme I below).[27] We performed 1-MeIm titrations to measure the equilibrium constants $K_1$ and $K_2$ for binding the first and second 1-MeIm to $Fe^{III}PP$ in 2% CTAB (50 mM Tris buffer, pH 9), using the method of Brault and Rougee.[23] This method requires knowledge of the spectrum of Fe(PP)(1-MeIm), which is not measurable directly; it was taken to be identical with that of FePP(2-MeIm). In particular, we measured the extinction coefficient of the 2-MeIm complex to be $\epsilon_{FePP(2\text{-}MeIm)}$ $1.48 \times 10^5$ $M^{-1}$ $cm^{-1}$ at 436.8 nm and assumed $\epsilon_{FePP(1\text{-}MeIm)} \equiv \epsilon_{FePP(2\text{-}MeIm)}$. The equilibrium constants were determined to be $K_1 = 118 \pm 35$ $M^{-1}$ and $K_2 = 139 \pm 42$ $M^{-1}$, which are quite low compared to those for bases in nonaqueous solution.[19,23]

The solubility of NO in neat 1-MeIm, measured by using the method described in the Experimental Section above, was found to be $s_{NO}$ = 3 mM/atm. The solubility of CO in 30% (v/v) 1-MeIm in aqueous Tris buffer at pH 9 was found to be $s_{CO}$ = 0.8 mM/atm.

**Equilibrium NO Binding.** Table I collects the results of Romberg and Kassner for the partial pressures ($P_{1/2}$) for 50% ligation by NO of FePP(1-MeIm) in 20% (v/v) 1-MeIm/aqueous buffer, the results of Geibel, et al., for $P_{1/2}$ for CO coordination to meso-heme-mono-4-(1-imidazoyl)butylamide monomethyl ester[22,4] and the $P_{1/2}$ for NO and CO binding to Hb and Mb.[8] Using these reported values of $P_{1/2}$, and the solubilities of the two diatomics determined here, we calculate the equilibrium constants for ligand binding ($K_L$) given in Table I. We note that the ratio of the affinities for the unconstrained porphyrins, $K_{NO}/K_{CO}$ = 740, is essentially indistinguishable from that for R-state Hb (~1100) but is 10-fold less than that for Mb (7500).

Table II. Rate Constants for NO and CO Binding to Five-Coordinate FePP

| heme | $k_s$, $M^{-1}$ $s^{-1}$ | $k_{-s}$, $s^{-1}$ | conditions and references |
|---|---|---|---|
| | NO | | |
| FePP(1-MeIm) | $1.8 \pm 0.7 \times 10^{8}$ [a,b] | $2.9 \times 10^{-4}$ [d] | this work, c |
| Hb(T) | $1.8 \times 10^{7}$ | $4.0 \times 10^{-3}$ | e |
| | | $7.0 \times 10^{-2}$ | |
| Hb(R) | $1.8 \times 10^{7}$ | $5.0 \times 10^{-5}$ | f |
| Mb | $1.7 \times 10^{7}$ | $1.2 \times 10^{-4}$ | g, 7 |
| | CO | | |
| Fe(porphyrin)(B) | $2–6 \times 10^{6}$ | | h |
| FePP(1-MeIm) | $1.8 \pm 0.7 \times 10^{6}$ [i] | $2.3 \times 10^{-3}$ [d] | this work, b |
| Hb(T) | $1.5 \times 10^{5}$ | $1.4 \times 10^{-1}$ | j |
| Hb(R) | $6.0 \times 10^{6}$ | $1.4 \times 10^{-2}$ | j |
| Mb[g] | $5.0 \times 10^{5}$ | $2.1 \times 10^{-2}$ [d] | g, 8 |

[a] Within experimental error, results with 20% and 30% (v/v) 1-MeIm are identical: $\kappa$ (eq 3) = $4.8 \pm 1.4 \times 10^5$ $M^{-1}$ $s^{-1}$ (20% MeIm) and $3.5 \pm 1.4 \times 10^5$ $M^{-1}$ $s^{-1}$ (30% MeIm). [b] Calculated from $\kappa$ (footnote a) by using eq 6 with $k_4 = 1 \times 10^9$ $M^{-1}$ $s^{-1}$, $K_1 = 118$, $K_2 = 139$ $M^{-1}$. [c] Aqueous buffer, pH 9.0, 20% (v/v) 1-MeIm and 30% (v/v) 1-MeIm are indistinguishable. [d] Calculated from $K_L = k_s/k_{-s}$, $K_L$ values from Table I, and included for illustrative purposes. [e] Aqueous buffer, pH 6, tuna hemoglobin, ref 10. Two T-state dissociation constants are observed. [f] Aqueous buffer, pH 8, tuna hemoglobin, ref 10. [g] Aqueous buffer, pH 7; sperm whale myoglobin, ref 7 and 8. [h] For references to the kinetic constants of a wide variety of five-coordinate heme models, see ref 2 and 11. [i] Calculated from $\kappa = 4.3 \pm 1.3 \times 10^3$ $M^{-1}$ $s^{-1}$, using eq 3 with $k_4 = 2 \times 10^8$ $M^{-1}$ $s^{-1}$ (ref 27), binding constants listed above. [j] Aqueous buffer, pH 6.6; Fe-Mn hybrid human hemoglobin, ref 9.

**Kinetics of NO Binding.** It is possible to choose a proper, low value for the equilibrium ratio [NO]/(1-MeIm] such that a heme solution in equilibrium is fully converted to Fe(PP)(1-MeIm)(NO) and yet immediately forms Fe(PP)(1-MeIm)$_2$ subsequent to photolysis. For example, under conditions of high [1-MeIm], namely, 20% or greater 1-MeIm, and low [NO], with $10^{-5} \leq$ [NO] $\lesssim 10^{-3}$ M, the static optical spectrum is that of Fe(PP)(1-MeIm)(NO). Photodissociation of FePP(1-MeIm)(NO) is then readily observed, and the kinetic difference spectrum is identical with the static difference [FePP(1-MeIm)$_2$ − FePP(1-MeIm)-(NO)] (Figure 1). Thus, the kinetic difference spectrum verifies that such conditions insure full formation of the initial six-coordinate FePP(1-MeIm)(NO) complex in the dark and also lead to formation of the bis(base) complex within the lifetime of the flash. The bis(base) complex returns to FePP(1-MeIm)(NO) in a pseudo-first-order process, with the observed rate contants $k_{obsd}$ accurately proportional to [NO] over the measured concentration range, $10^{-5} \leq$ [NO] $\leq 10^{-3}$ M (Figure 2). The second-order rate constants, for NO binding, $\kappa_{NO} = k_{obsd}/$[NO], for the solution conditions employed were calculated and are presented in a footnote to Table II. For purposes of comparison we performed the same experiment using FePP(1-MeIm)(CO) (pH 9, 30% (v/v) 1-MeIm) and also observed a pseudo-first-order return of FePP(1-MeIm)$_2$ to FePP(1-MeIm)(CO); the second-order rate constant is presented in a footnote to Table II.

A bis(base) ferroheme complex formed upon photolysis undergoes rapid equilibration with monobase and unliganded heme,

(26) Brunori, M.; Giacometti, G. M.; Antonini, E.; Wyman, J. *Proc. Natl. Acad. Sci. U.S.A.* **1973**, *70*, 3141–3144.

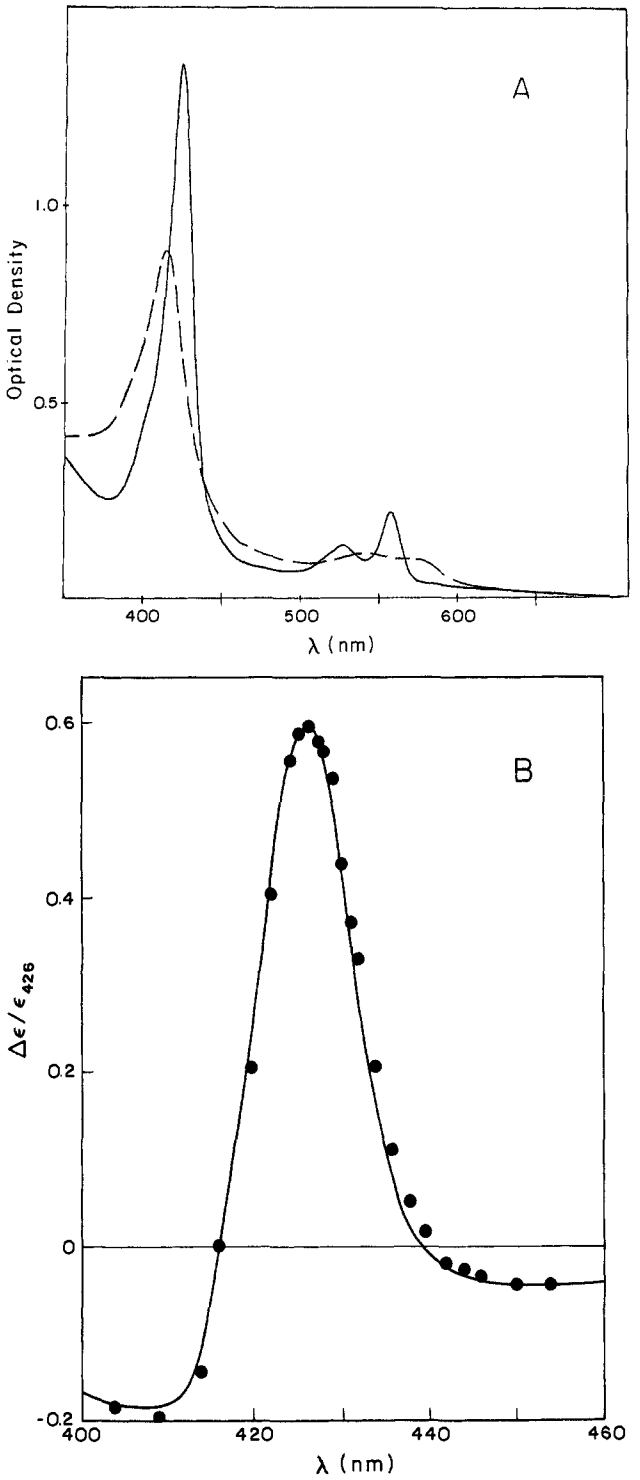


**Figure 1.** (A) Absorption spectra of $Fe^{III}PP(1\text{-}MeIm)_2$ (—) and $Fe^{II}PP(1\text{-}MeIm)(NO)$ (- - -) in 30% v/v 1-MeIm, 50 mM aqueous Tris buffer, pH 9, [NO] ≈ $10^{-4}$ M, 20 °C. (b) Static and kinetic difference spectra of [FePP(1-MeIm)$_2$ − FePP(1-MeIm)(NO)]; conditions as in A. Kinetic spectrum has been normalized at $\Delta\epsilon_{max}$, and scaling is based on extinction coefficients reported in ref 22: (—) static difference; (●) kinetic difference.

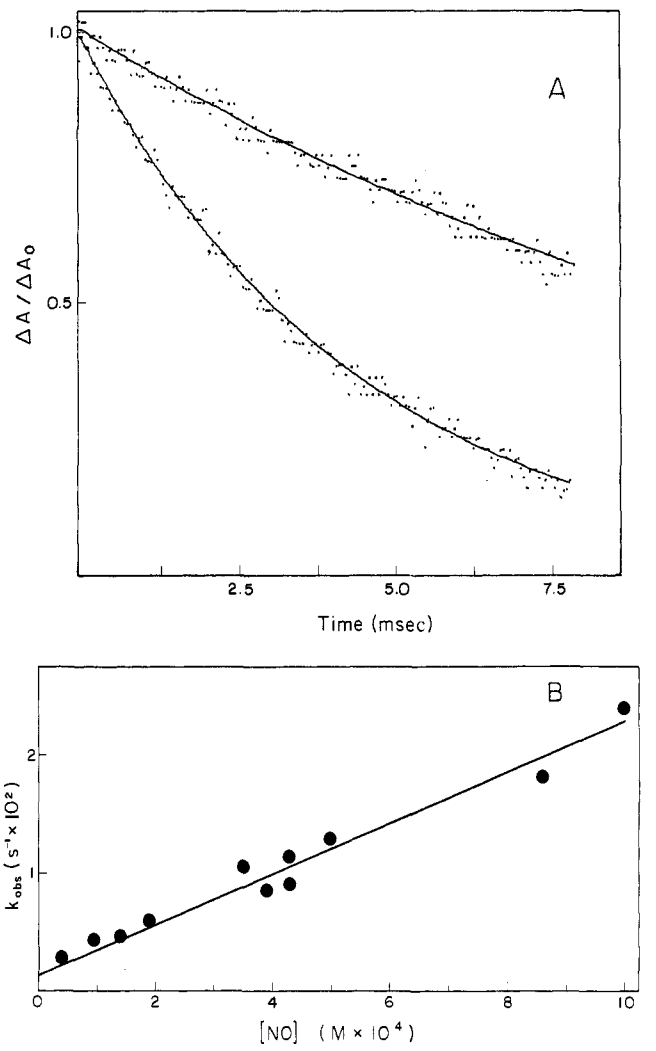


**Figure 2.** (A) Observed pseudo-first-order binding of NO to FePP(1-MeIm)$_n$, $n$ = 0, 1, according to Scheme I. Points are data; lines are fit by a nonlinear least-squares first-order decay scheme: (lower trace) [FePor] ~ $5 \times 10^{-6}$ M, [B] = 3.8 M, [NO] = $5 \times 10^{-4}$ M, 20 °C; (upper trace) same sample, [NO] = $1.5 \times 10^{-4}$ M. (B) Plot of $k_{obsd}$ vs. [NO]. Each point represents different sample. Non-zero intercept is within experimental error given uncertainty in [NO] and $k_{obsd}$.

Scheme I

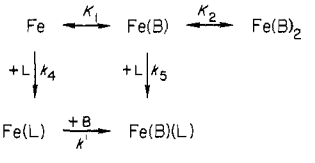


and the observed rebinding of a diatomic, L, to form FePP(1-MeIm)(L) results from a combination of L with both the four- and five-coordinate porphyrin species (Scheme I).[27] Here the porphyrin abbreviation has been suppressed. $K_1$ and $K_2$ are the base binding constants, and $k_4$ and $k_5$ are the second-order ligand binding rates. Although rebinding of NO is more rapid than for CO, not only is this scheme the same for both systems but, in fact, we rely heavily upon the formation of the bis(base) complex in order to slow the NO rebinding process to a rate observable on the time scale of our experiments. Results presented below verify that loss of L after rebinding can be neglected in the analysis.

White et al.[27] showed that if ligand addition is rate limiting and proceeds via Scheme I, then the observed ligand rebinding rate is proportional to [L], as observed both for L = CO and NO, and obeys an equation that may be written:

$$\kappa_L\Sigma \equiv \frac{k_{obsd}\Sigma}{[L]} = k_4 + k_5K_1[B] \qquad (3)$$

where $\Sigma = 1 + K_1[B] + K_1K_2[B]^2$. Ordinarily, the kinetic constants are obtained from eq 3 by measuring the binding rates as a function of base concentration as [B] is varied over a fairly wide range, typically 5-fold or more.[27,20] In our experiments, a minimum of 20% 1-MeIm is required in order to insure the predom-

(27) White, D. K.; Cannon, J. B.; Traylor, T. G. *J. Am. Chem. Soc.* **1979**, *101*, 2443–2454.

Table III. Quantum Yields for NO Photorelease from FePP(1-MeIm)(NO)[a]

| λ excitation, nm | T, °C | % 1-MeIM (v/v) | $\Phi_{NO}$[b] |
|---|---|---|---|
| 337.1[c] | 20 | 30 | 0.07 |
| 590[d] | 20 | 30 | 0.06 |
| 590[d] | 20 | 100 | 0.08 |
| α–β[e] | 20 | 30 | 0.08 |
| α–β[e] | 0 | 30 | 0.03 |

[a] Aqueous buffer, pH 9.0. [b] ±30%. [c] NRG nitrogen laser, [NO] = $2 \times 10^{-4}$ M. [d] Electrophotonics unmodelocked flash-lamp-pumped rhodamine-6-G dye laser; $\Phi_{NO}$ invariant over the range $10^{-3}$ M ≥ [NO] ≥ $10^{-5}$ M. [e] Sunpak photographic flash screened with Corning 3-71 filter, [NO] = $2 \times 10^{-4}$ M.

inance of six-coordinate FePP(1-MeIm)(NO) in solution;[22] even with a 10% 1-MeIm solution, optical spectra show the presence of an appreciable amount of five-coordinate FePP(NO). Since this species is also photolabile, analysis of rebinding kinetics and quantum yields becomes complicated in its presence. Therefore, study of the six-coordinate FePP(1-MeIm)(NO) and kinetic analysis according to Scheme I employed 20–30% 1-MeIm (v/v), a range of concentrations too small to allow an accurate determination of $k_4^{NO}$ as well as $k_5^{NO}$ from eq 3. However, at these high base concentrations, NO addition to the four-coordinate porphyrin, $k_4$, contributes only minimally to the observed rebinding rate, and a calculation of $k_5$ from eq 3 is quite insensitive to the choice of $k_4$ within the plausible range $k_4^{NO} = 10^8$–$10^{10}$ $M^{-1}/s^{-1}$. Therefore, we obtained $k_5^{NO}$ directly from the second-order rate constants, $\kappa_{NO}$ (Table II), using eq 3, our measured $K_1$ and $K_2$, and an estimated value of $k_4^{NO} = 10^9$ $M^{-1}$ $s^{-1}$. The principal uncertainties in $k_5^{NO}$ involve the uncertainties in $K_1$, $K_2$, and [NO], and not $k_4^{NO}$. Since $k_4^{CO}$ is known,[27] the second-order CO binding rate (Table II, footnote) could be used directly in eq 3 to obtain $k_5^{CO}$.

Table II lists the rate constants, $k_5^L$, for NO and CO binding to Fe(PP)(1-MeIm). The NO rate constant is 2 orders of magnitude larger than that for CO ($k_5^{NO}/k_5^{CO} = 95$). As support of the analysis procedure, we note that $\kappa^{NO}/\kappa^{CO} = 81 \sim k_5^{NO}/k_5^{CO}$, as required by eq 3 when binding to the four-coordinate Fe(PP) contributes minimally. Table II also includes the rate constants for NO and CO addition to Mb and to T- and R-state Hb. Whereas the protein CO on-rates vary among the three protein forms, the NO on-rates do not. For illustrative purposes, the equilibrium (Table I) and rate constants were used to estimate ligand dissociation rate constants, $k_{-5}$ (Table II).

**Quantum Yield: FePP(1-MeIm)(NO).** Quantum yields for NO photodissociation were obtained by using three actinic sources, the $N_2$ laser, rhodamine dye laser, and photographic flash. Because the NO rebinding rate constant is extremely large, FePP(1-MeIm)(NO) is readily observed to photodissociate only under conditions of relatively high [1-MeIm] and low [NO]. Therefore, the quantum yield for NO photodissociation was measured for FePP(1-MeIm)(NO) both in 30% and 100% 1-MeIm, with varying NO concentrations, [NO] ~ $10^{-3}$–$10^{-5}$ M. The quantum yield was invariant under these conditions (Table III), indicating that no photoproduct was lost due to *second-order* NO binding processes.

When the nitrogen laser is used as the photolytic source, excitation is monochromatic at 337 nm, to the blue of the Soret peak, and $\Phi_{NO}$ (337), given in Table III, is obtained from eq 1 and 2 directly. At the other extreme of the absorption spectrum, the red tail of the α band, and dye laser provides nearly monochromatic excitation but does have a finite, though small, bandwidth with $\lambda_{max}$ 590 nm. In this case, 2 should be integrated over the narrow wavelength range of laser emission in order to use eq 1 to obtain $\Phi_{NO}$. However, a rough integration of the extinction profiles of MbCO and FePP(1-MeIm)(NO) over the wavelength band covered by the laser emission indicated that $I(\lambda)\epsilon(\lambda)$ for the two species was nearly the same. The slope, ω, obtained from a plot of eq 1 vs. $I$ was therefore normalized to that of MbCO ($\Phi$ = 1) without further correction in order to obtain $\Phi_{NO}$ ($\lambda_{ex} \approx 590$) (Table III, Figure 3).

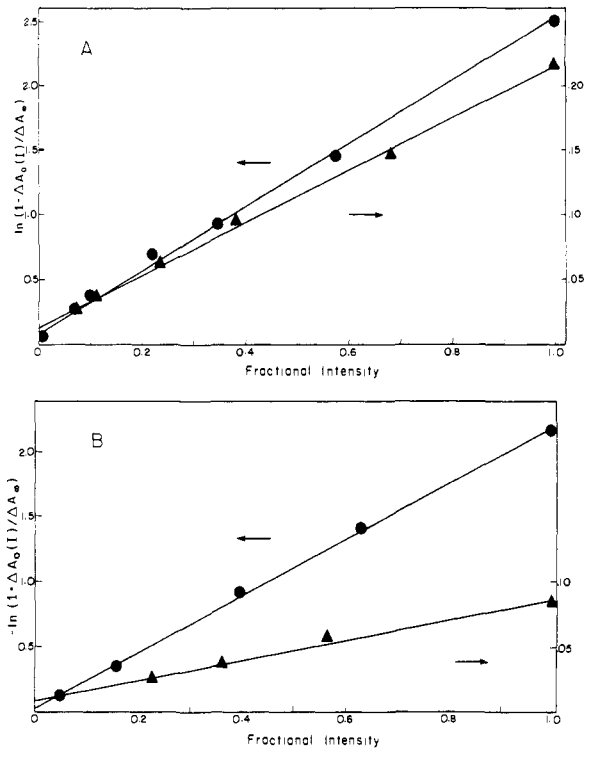


**Figure 3.** (A) NO photorelease quantum yield plot according to eq 1 for $Fe^{II}$PP(1-MeIm)(NO) in 100% 1-MeIm and for MbCO. Straight lines are generated by linear least-squares fit. Conditions: flash source, R6G-pulsed dye laser; 20 °C, [FePor] ~ $8 \times 10^{-6}$ M, [NO] = $2 \times 10^{-4}$ M. (Δ) FePP(1-MeIm)(NO); (●) MbCO. (B) NO photorelease quantum yield plot according to eq 1 for $Fe^{II}$PPNO in 1 M 2-MeIm (aqueous tris, pH 9) and for MbCO. Conditions: flash source, R6G-pulsed dye laser; 20 °C, [FePor] ~ $5 \times 10^{-6}$ M, [NO] = $3 \times 10^{-4}$ M. (▲) FePPNO; (●) MbCO.

The photographic flash, screened by a Corning 3-71 sharp cut, long-pass yellow filter (50% transmission λ 440 nm), illuminates both FePP(1-MeIm)(NO) and MbCO over the entire α–β region. The quantum yield for CO photorelease from MbCO is unity and is wavelength independent through this entire region.[12] We define $\bar{\Phi}$ for FePP(1-MeIm)(NO) as the average quantum yield for excitation at all wavelengths in the α–β region

$$\int_{\alpha-\beta} \Phi(\lambda)\epsilon(\lambda)i(\lambda)\, d\lambda \equiv \bar{\Phi} \int_{\alpha-\beta} \epsilon(\lambda)i(\lambda)\, d\lambda$$

After integration of the extinction profiles of both species over the same limits, plots according to eq 1 were compared to obtain $\bar{\Phi}_{NO}$.

Quantum yields for NO photorelease from FePP(1-MeIm)(NO) for the three actinic sources are collected in Table III. The two values obtained with long- and short-wavelength monochromatic excitation, as well as the average value, $\bar{\Phi}$, are the same within experimental error, $\bar{\Phi} = 0.07 \pm 0.03$, indicating that $\Phi_{NO}$ is wavelength independent over the wavelength range encompassing both the α, β, and Soret adsorption bands.

The temperature dependence of the quantum yield for NO photorelease was probed by measuring $\bar{\Phi}$ at 0 °C. Although it was only convenient to use the photographic flash as the actinic source, the use of this broadband source is justified by the correspondence at 20 °C between $\bar{\Phi}_{NO}$ and the $\Phi_{NO}$ obtained with monochromatic excitation. The $\bar{\Phi}_{NO}$ at 0 °C was roughly half the value obtained at room temperature (Table III).

**Quantum Yield: FePPNO.** Even at very low [NO] we were unable to do more than verify qualitatively the photolability of FePPNO. The observed transients were small and noisy, with recombination occurring nearly within the lifetime of the photolyzing flash. The success of the method of trapping the photofragments produced in the photolysis of six-coordinate FePP-

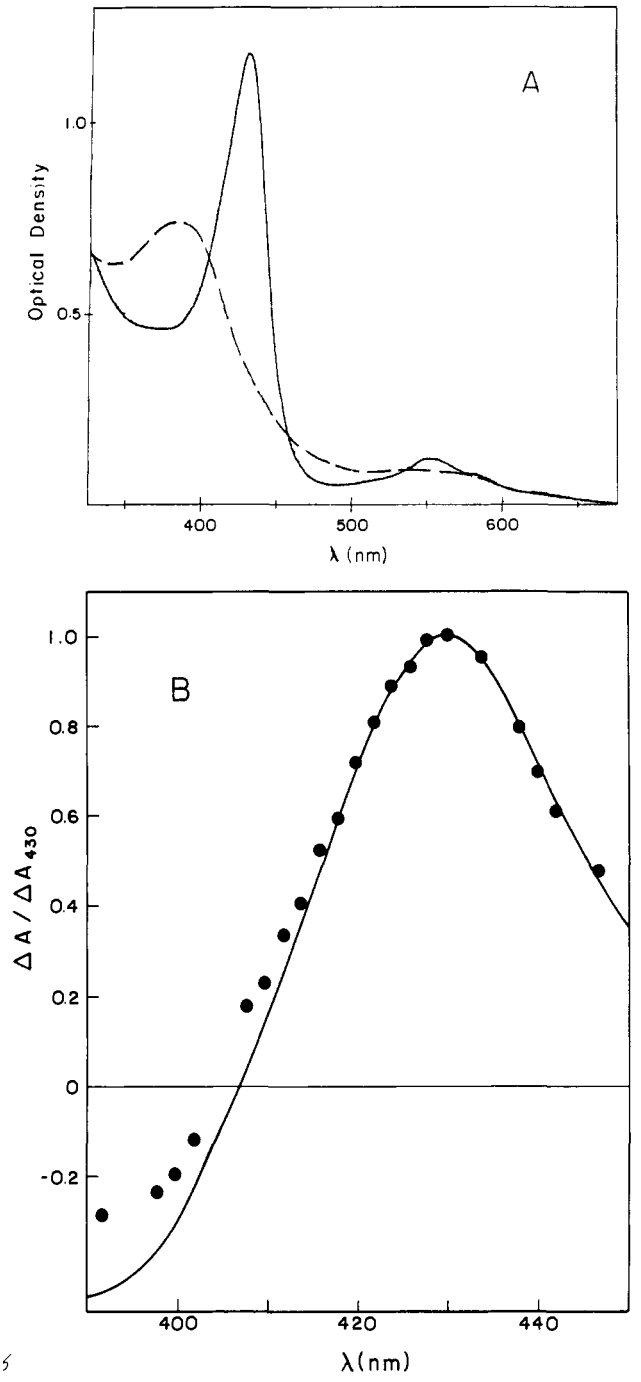


**Figure 4.** (A) Absorption spectra of $Fe^{II}PP(2\text{-MeIm})$ (—) and $Fe^{II}PP$-NO (- - -) in 0.5 M 2-MeIm, aqueous Tris, pH 9, 20 °C, [NO] = $2 \times 10^{-3}$ M. (B) Static and kinetic difference spectra of [FePP(2-Me-Im) - Fe(II)PP(NO)] under conditions described above. Spectra have been normalized at $\Delta A_{max}$: (—) static difference; (●) kinetic difference.

(1-MeIm)(NO) suggested that a similar system be developed for trapping the photogfragments of FePP(NO) photolysis. It has been shown that only a single 2-MeIm can bind to heme, forming FePP(2-MeIm).[23] Steric hindrance by the methyl group in the 2-position prevents coordination by a second base molecule. Structural studies of stable five-coordinate FePor(NO) species have shown that the Fe of FePor(NO) is displaced from the porphyrin plane toward the NO,[28] and the competing steric requirements of these two ligands suggested that 2-MeIm would not bind to FePor(NO). Indeed, addition of NO (1 atm) to $Fe^{II}PP(2\text{-MeIm})$ in solution with [2-MeIm] = 1 M results in complete conversion to the five-coordinate FePP(NO) (Figure 4).

(28) Scheidt, W. R.; Frisse, M. E. *J. Am. Chem. Soc.* **1975**, *97*, 17–21.

Furthermore, as expected, the apparent photolability of FePP(NO) was increased by the addition of 2-MeIm. Comparison of the static [FePP(2-MeIm)-FePP(NO)] difference spectrum with the flash difference spectrum showed that the $Fe^{II}PP$ photofragment produced upon photolysis of FePP(NO) in the presence of 2-MeIm was trapped as FePP(2-MeIm) (Figure 4). Although the photolysis transients were still small, and recombination extremely fast, we were able to estimate $\Phi \approx 0.04$, both with [2-MeIm] = 0.5 and 1.0 M. This value, which is comparable to that for FePP(B)(NO), is of course a lower limit for the true quantum yield for photorelease of NO from FePP(NO), and rapid recombination may yet be lowering the $\Phi$ observed on the microsecond time scale of our experiments. Nevertheless, the lack of variation in $\Phi$ over the small range of [2-MeIm] employed suggests the value of reasonably free of artifacts associated with NO recombination through *second-order* processes.

## Discussion

We have measured the quantum yield for NO photodissociation from the six-coordinate nitrosylferroheme model compound Fe(PP)(1-MeIm)(NO) and the rate constant for NO binding to the five-coordinate compound, $Fe^{II}PP(1\text{-MeIm})$. Each quantity is substantially greater than the corresponding value for the heme prosthetic group incorporated into the protein matrix of Hb (Tables II, III). The results for free and incorporated heme both can be understood within a simplified reaction scheme for binding and photorelease.[10,18] Here, Fe represents either the unliganded heme in solution or in the protein, (Fe, L) represents the heme–ligand encounter pair, either in a solvent cage or embedded in the heme pocket, and $\Phi_1$ represents the intrinsic quantum yield for photodissociation. The second-order rate constant, $k_d$, represents either diffusive encounter of ligand and heme model or diffusion of the ligand into the heme binding site; $k_{-1}$ is the rate constant for the return of ligand to the solvent and $k_2$ the rate constant for the bond formation step. $\Phi_1$ represents the intrinsic quantum yield for photodissociation; for both L = CO and NO, the spontaneous bond-breaking process can be neglected because the rate constants for ligand release are quite low (Table II).

**Scheme II**

$$\text{Fe} + \text{L} \underset{k_{-1}}{\overset{k_d}{\rightleftharpoons}} (\text{Fe, L}) \underset{\Phi_1}{\overset{k_2}{\rightleftharpoons}} \text{Fe–L}$$

According to Scheme II, the observed second-order rate constant for the binding of diatomic L to the heme within the protein is given by

$$k_{obsd}^{L} = \frac{k_2 k_d}{k_{-1} + k_2} = \frac{k_d}{1 + (k_2/k_{-1})^{-1}} \tag{4}$$

For example, when $k_2/k_{-1} \gg 1$, then $k_{obsd}^{L} \rightarrow k_d$, and diffusive formation of (Fe, L) controls the rate of reaction; once (Fe, L) has formed, the probability of bond formation is overwhelmingly greater than that of nonproductive disassociation. The apparent quantum yield for photodissociation is given by

$$\Phi_{app} = \frac{\Phi_1}{1 + (k_2/k_{-1})} \tag{5}$$

In particular, when $k_2/k_{-1} \gg 1$, then $\Phi_{app} \ll \Phi_1$. Thus, for a given system, both $k_{obsd}$ and $\Phi_{app}$ are controlled by the ratio of nonproductive and productive decay rates for the (Fe, L) encounter pair; namely, $k_2/k_{-1}$. More complicated schemes, involving several intermediates, have been developed in the elegant studies of Frauenfelder and co-workers,[29-31] but Scheme II is adequate for

(29) Alberding, N.; Austin, R. H.; Chan, S. S.; Eisenstein, L.; Frauenfelder, H.; Gunslas, I. C.; Nordlund, T. M. *J. Chem. Phys.* **1976**, *65*, 4701–4711.

(30) Austin, R. H.; Beeson, K. W.; Eisenstein, L.; Frauenfelder, H.; Gunslas, I. C. *Biochemistry* **1975**, *14*, 5355–5373.

(31) Doster, W.; Beece, D.; Bowne, S. F.; DiIorio, E. E.; Eisenstein, L.; Frauenfelder, H.; Reinisch, L.; Shyamsunder, E.; Winterhalter, K. H.; Yue, K. T. *Biochemistry*, submitted for publication.

our purposes. In fact, the results of a sophisticated kinetic treatment, which tries to model in detail the binding of CO to protoheme in solution,[32] can be shown to correspond identically with eq 4 and 5. We first discuss our model studies and then use Scheme II to relate them to the protein results.

**FePP Model Compounds.** The rate constants, $k_5$, for NO and CO binding to the five-coordinate $Fe^{II}PP(1\text{-MeIm})$ complex are given in Table II along with the corresponding values for both R- and T-state hemoglobin. The rate constants for CO association to unconstrained model system agree within experimental uncertainties with that for CO binding to R-state hemoglobin (Table II).[9,11] Thus, the CO binding rate is not suppressed by the protein in its high-affinity state. In the low-affinity T state, hemoglobin exhibits a rate of CO association that is lowered ~40-fold from that of R-state hemoglobin and of the unhindered model.[9] Myoglobin, which exhibits a high ligand affinity, also shows a binding rate that is reduced from the unconstrained value and similar to that of T-state hemoglobin.[8]

The value of $k_5^{NO} \sim 2 \times 10^8$ $M^{-1}$ $s^{-1}$ for a five-coordinate solution heme is 100-fold greater than $k_5^{CO}$ (Table II) and approaches $k_d^S$, the value for a diffusion-controlled reaction. A "typical" upper limit for the rate constant of a bimolecular diffusion-controlled reaction between two neutral molecules in aqueous solution is[33] $k_d^S \sim 4 \times 10^9$ $M^{-1}$ $s^{-1}$. Orientation factors must reduce the reaction of NO with FePP(B) by a factor of 4 at the least (2× for NO orientation; 2× because only one side of the heme is available for coordination), and Reisberg and Olson[34] estimate that the rate constant for a diffusion-controlled reaction between a diatomic and protoheme in solution should be attenuated by a factor of 12 (2× for NO; 6× for access to Fe). If the range $4 \times 10^8$ $M^{-1}$ $s^{-1} < k_d^S < 1 \times 10^9$ $M^{-1}$ $s^{-1}$ is accepted as reasonable; then $k_5^{NO}$ is lower by a factor of perhaps 2–5, indicating that NO binding to the free five-coordinate heme approaches but probably does not reach the diffusion-controlled limit. In terms of Scheme II, and eq 4, this factor of 2–5, though primarily of heuristic value, corresponds to an approximate value for the rate ratio of $(k_2/k_{-1})$ ~0.5–0.2. In other words, an (Fe, NO) encounter pair in a solvent cage is somewhat more likely to separate into reactants than it is to undergo bond formation. In contrast, $k_5^{CO}$ for FePP(1-MeIm) is 100-fold less than $k_d^S$, and (eq 4) separation of the (Fe, CO) pair is over 100-fold more likely than bond formation. The rate for NO binding to the four-coordinate porphyrin, $k_4$, which we cannot determine accurately, appears in fact to represent the diffusion limit, with $k_2/k_{-1} > 1$ and bond formation the probable outcome of encounter-pair formation. Interestingly, the rute constant for CO binding to a four-coordinate heme ($2 \times 10^8$ $M^{-1}$ $s^{-1}$)[27] is equal to that of NO binding to a five-coordinate heme (Table II) and thus can be analyzed identically.

The quantum yields for NO photodissociation from FePP(1-MeIm)(NO) using three photolysis sources under various experimental conditions are given in Table III. The equivalence of $\Phi_{app}^{NO}$ for FePP(1-MeIm)(NO) in solutions of 30% (v/v) and 100% 1-MeIm indicates that no photoproduct is being lost due to *second-order* NO-binding processes. At room temperature the quantum yield, $\Phi_{app}^{NO}$ (20 °C) = 0.07, is wavelength independence over the range encompassing the $\alpha$, $\beta$, and Soret absorption bands. Inserting into eq 5 the estimate, $k_2/k_{-1} \sim 0.5$–0.2, obtained above, gives $\Phi_1 \sim 0.08$–0.1. Thus, it appears that cage recombination following photodissociation of NO from FePP(1-MeIm)(NO) lowers the observed quantum yield only by ~20–30%. The value of $\Phi_1$ is far higher than that for nitrosylferrohemoproteins ($\Phi_{app}$ ~ 0.01–0.001),[12,13] thus corroborating the observation of Morris and Gibson, who showed that the quantum yield for nitrosyl dimethyldeuteroheme disulfonate $\Phi = 0.15$.[10] These values are apparently still low enough to support the distinction of compounds with $r \geq 7$ from those with $r = 6$ and $\Phi \approx 1$.[14] Confirmation of these estimates by direct observation on a nanosecond time scale is planned.

The temperature variation of $\Phi_{app}^{NO}$ is unlikely to arise from changes in $\Phi_1$ and almost certainly reflects a temperature dependence in $k_2/k_{-1}$. Taking $\Phi_1 \sim 0.1$, the 2-fold reduction in apparent quantum yield upon cooling to 0 °C relative to the rate of reactant separation at 0 °C has decreased to the point that bond formation is about as likely a fate for (Fe, NO) as is separation.

In the case of the five-coordinate nitrosyl complex FePP(NO), we can only put broad limits on the value of $k_2/k_{-1}$. Here $\Phi_{app} \sim 0.04$; if this is assumed to be a lower limit to $\Phi_1$, then 5 yields as an upper limit $k_2/k_{-1} \leq 25$.

**Hemoproteins.** The rate constant for NO binding to hemoglobin or myoglobin is ~10 times lower than the comparable value for NO binding to the five-coordinate protoporphyrin model compound (Table II). Since there is no allosteric differentiation between NO binding to the protoheme of the R and T states of hemoglobin, or of myoglobin,[10] incorporation of protoheme into the protein thus appears to restrict NO access to the prosthetic group, but the effect is not sensitive to protein quaternary structure. We now show that this result and the low quantum yield for NO photorelease from NOHb ($\Phi_{app} \sim 10^{-3}$) are general consequences of sequestering the heme within a protein and both can be understood through use of Scheme II.

Szabo,[13] following the method of Hill,[35] notes that merely embedding a heme into a protein pocket restricts access to it and suggests as an upper limit $k_d^P \sim 5 \times 10^8$ $M^{-1}$ $s^{-1}$ for the rate constant for diffusion of a diatomic ligand into a hemoprotein binding site. A tighter bound is the rate constant for oxygen quenching of the porphyrin triplet state in ZnPP- or PP-substituted myoglobin $k_Q \sim 1$–$2 \times 10^8$ $M^{-1}$ $s^{-1}$.[36-38] Phosphorescence quenching represents the diffusion limit of Scheme II, with $k_{-1}/k_2 \rightarrow 0$, since quenching occurs upon interaction between oxygen and the Zn-porphyrin prosthetic group, $k_{-1}$ does not contribute at all to the rate description. However, the rate of phosphorescence quenching also clearly overestimates the rate of diffusion to the ligand binding site, because oxygen has a large effective quenching radius and also can quench by interaction with the porphyrin ring rather than the metal center. Therefore, for binding a diatomic to the heme iron of a hemoprotein, a plausible estimate for the diffusion rate constant in Scheme II is perhaps $k_d^P \sim 5$–$10 \times 10^7$ $M^{-1}$ $s^{-1}$. Thus, a diffusion-controlled process will be slowed 10-fold, namely, $k_d^P/k_d^S \sim 0.10$, merely upon incorporation of the heme into the heme pocket.

The observed rate constants for NO binding to Hb (Table II) are quite comparable to the estimate of $k_d^P$. Within Scheme II, $k_{obsd}^L$ can approach $k_d^P$ only when $k_2/k_{-1} \gg 1$ (eq 4). This contrasts with the result $k_2/k_{-1} < 1$ for the model and must reflect a hindrance to loss of ligand from the heme pocket (reduced $k_{-1}$) that is analogous to the reduction in $k_\alpha$. The large rate ratio in turn requires (eq 5) that germinate recombination within the cage provided by the heme pocket sharply reduces the observed photodissociation quantum yield: $\Phi_{app}/\Phi_1 \sim 1/(k_2/k_{-1}) \ll 1$. Indeed, quantum yields for NO photorelease from HbNO are low,[12] $\Phi_{app} \sim 10^{-3}$, compared with $\Phi_{app} \sim 0.1$ for the model compound. Since it is unlikely that $\Phi_1$ for a heme-ligand system is changed by incorporation into a protein environment, we may take $\Phi_1 \sim 0.1$ as for the model; the reduced hemoprotein quantum yield then requires $k_2/k_{-1} \sim 10^2$ for NO binding to Hb and Mb, consistent with the kinetic results. Thus, in contrast to the weak cage effect inferred for an (Fe, NO) pair in solution, hemoprotein ligand binding and quantum yield measurements indicate that restricted diffusion into and out of the heme pocket makes it over 100 times more likely for a NO molecule in the pocket to bind than to escape.

Further application of Scheme II to the nanosecond photolysis studies of HbCO and $HbO_2$ by Duddell, et al.[18] lead to the es-

(32) Peak, D. *J. Chem. Phys.* **1982**, *76*, 3792–3798.
(33) Amdur, I.; Hammes, G. G. "Chemical Kinetics, Principles and Selected Topics"; McGraw-Hill: New York, 1966; pp 60–64.
(34) Reisberg, P. I.; Olson, J. S. *J. Biol. Chem.* **1980**, *255*, 4151–4158.
(35) Hill, T. L. *Proc. Natl. Acad. Sci. U.S.A.* **1975**, *72*, 4918–4922.
(36) Zemel, H.; Hoffman, B. M. *J. Am. Chem. Soc.* **1981**, *103*, 1192–1201.
(37) Alpert, B.; Lindquist, L. *Science (Washington, D.C.)* **1974**, *187*, 836–837.
(38) Austin, R. H.; Chan, S. S. *Biophys. J.* **1978**, *24*, 175–182.

timates $k_2/k_{-1} \sim 0.4$ for CO and $k_2/k_{-1} \sim 1$ for $O_2$. In this regard, as in the cooperativity of ligation, the behavior of CO and of $O_2$ in Hb is comparable, differing markedly from that of NO.

**Acknowledgment.** This work was supported by the National Science Foundation (PCM 7681304).

**Registry No.** FePP(1-MeIm)(NO), 76759-31-4; FePP(NO), 54854-55-6; FePP(1-MeIm), 70085-59-5; FePP(1-MeIm)$_2$, 78261-95-7; FePP(2-MeIm), 70085-59-5.

# Total Synthesis of (±)-14-Epicorynoline, (±)-Corynoline, and (±)-6-Oxocorynoline

**Mark Cushman,* Aziz Abbaspour, and Yash Pal Gupta**

*Contribution from the Department of Medicinal Chemistry and Pharmacognosy, School of Pharmacy and Pharmacal Sciences, Purdue University, West Lafayette, Indiana 47907.*
*Received June 7, 1982*

**Abstract:** The condensation of piperonylidenemethylamine (**15**) with 3,4-(methylenedioxy)-7-methylhomophthalic anhydride (**14**) has been utilized as the key step in a total synthesis of the naturally occurring hexahydrobenzo[*c*]phenanthridine alkaloids (±)-corynoline (**1**), (±)-6-oxocorynoline (**2**), and (±)-14-epicorynoline (**3**). The production of each of the desired diastereomers **16** and **17** was maximized under certain specified reaction conditions. An unusual fragmentation reaction was discovered during the conversion of the diazo ketone **20** to the substituted 1(2*H*)-isoquinolone **22** under acidic conditions. Two conformers of the tetracyclic intermediate **30** were detected at room temperature by 470-MHz $^1$H NMR spectroscopy. The identity of (+)-isocorynoline with (+)-14-epicorynoline was also demonstrated.

(±)-Corynoline,[1] (+)-corynoline (**1**),[2] 6-oxocorynoline (**2**),[3] and

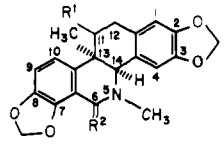

**1**, $R^1$ = α-OH; $R_2$ = $H_2$
**2**, $R^1$ = α-OH; $R_2$ = O
**9**, $R^1$ = β-OH; $R_2$ = $H_2$

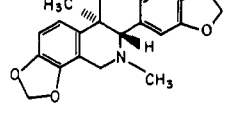

**3**, R = α-OH
**4**, R = β-OAc
**5**, R = α-OAc
**6**, R = β-OAc
**31**, R = β-OH
**32**, R = β-$OSO_2CH_3$
**34**, R = H

(+)-14-epicorynoline (**3**)[1,4] are benzophenanthridine alkaloids that have been isolated from *Corydalis incisa*. The structure **1** of (±)-corynoline was proposed in 1963 after contemplation of the results of chemical degradation studies, spectroscopic evidence, and biosynthetic considerations.[5] This structure assignment was later confirmed by an X-ray analysis of the *p*-bromobenzoate.[6] The absolute configuration of (+)-corynoline (**1**) was established by chemical correlation with (+)-14-epicorynoline (**3**),[2,7] the absolute configuration of which was proven by X-ray analysis of the bromoacetate.[8] At the outset of the present study the structural identities of (+)-isocorynoline and (+)-acetylisocorynoline appeared to be the subject of some confusion. In fact, (+)-acetylisocorynoline had appeared in the literature as three different structures, **4**,[9] **5**,[3] and **6**.[10]

Considerable effort has already been directed toward the total synthesis of the naturally occurring BC cis-fused hexahydrobenzo[*c*]phenanthridine alkaloids. The first synthesis of (±)-chelidonine (**7**) was executed by using the intramolecular Diels–Alder reaction of an *o*-quinodimethane derived from a benzocyclobutene.[11] More recently, the photocyclization of enamides was exploited during a total synthesis of (±)-corynoline (**1**), (±)-12-hydroxycorynoline (**8**), and (±)-11-epicorynoline (**9**).[12] Significant work has also been done on the chemical transformation of certain 13-methylprotoberberine alkaloids to analogues of the naturally occurring *cis*-13-methylbenzophenanthridines.[13] Other analogues of corynoline (**1**) have been prepared from homophthalimide derivatives.[14] However, very little work has been reported on the total synthesis of the naturally occurring BC trans-fused alkaloid 14-epicorynoline (**3**). We recently reported a total synthesis of (±)-chelidonine (**7**) that was based on the

(1) Tani, C.; Takao, N. *Yakugaku Zasshi* **1962**, *82*, 594.
(2) Takao, N.; Kamigauchi, M.; Iwasa, K. *Tetrahedron* **1979**, *1977*.
(3) Nonaka, G.; Nishioka, I. *Chem. Pharm. Bull.* **1975**, *23*, 521.
(4) Kametani, T.; Ihara, M.; Honda, T. *Phytochemistry* **1971**, *10*, 1881.
(5) Takao, N. *Chem. Pharm. Bull.* **1963**, *11*, 1306, 1312.
(6) Kametani, T.; Honda, T.; Ihara, M.; Shimanouchi, H.; Sasada, Y. *Tetrahedron Lett.* **1972**, 3729.
(7) Takao, N.; Bersch, H.-W.; Takao, S. *Chem. Pharm. Bull.* **1973**, *21*, 1096.
(8) Takao, N.; Kamigauchi, M.; Iwasa, K.; Tomita, K.; Fujiwara, T.; Wakahara, A. *Tetrahedron Lett.* **1974**, 805.
(9) Nonaka, G.; Okabe, H.; Nishioka, I.; Takao, N. *Yakugaku, Zasshi* **1973**, *93*, 87.
(10) Shamma, M.; Moniot, J. L. "Isoquinoline Alkaloids Research, 1972–1977"; Plenum Press: New York, 1978; p 271.
(11) Oppolzer, W.; Keller, K. *J. Am. Chem. Soc.* **1971**, *93*, 3836. An improved version of this synthesis was recently communicated: Oppolzer, W. *Heterocycles* **1980**, *14*, 1615.
(12) Ninomiya, I.; Yamamoto, O.; Naito, T. *J. Chem. Soc., Perkin Trans. I* **1980**, 212.
(13) Onda, M.; Yuasa, K.; Okada, J.; Kataoka, K.; Abe, K. *Chem. Pharm. Bull.* **1973**, *21*, 1333. Onda, M.; Yuasa, K.; Okada, J. *Ibid.* **1974**, *22*, 2365. Onda, M.; Harigaya, Y.; Horie, J. *Heterocycles* **1977**, *8*, 89. Onda, M.; Yamaguchi, H., Harigaya, Y. *Chem. Pharm. Bull.* **1980**, *28*, 866.
(14) Iida, H.; Endo, I.; Narimiya, M.; Kikuchi, T. *Heterocycles* **1980**, *14*, 1325.

0002-7863/83/1505-2873$01.50/0 